

Tidal Warping and Precession of Be Star Decretion Discs

Rebecca G. Martin^{1*}, J. E. Pringle², Christopher A. Tout² and Stephen H. Lubow¹

¹*Space Telescope Science Institute, 3700 San Martin Drive, Baltimore, MD 21218, USA*

²*University of Cambridge, Institute of Astronomy, The Observatories, Madingley Road, Cambridge, CB3 0HA, UK*

ABSTRACT

Rapidly rotating Be stars are observed as shell stars when the decretion disc is viewed edge on. Transitions between the two implies that the discs may be warped and precessing. Type II X-ray outbursts are thought to occur when the warped disc interacts with the fast stellar wind. We suggest that tides from a misaligned companion neutron star can cause the observed effects. We make numerical models of a Be star decretion disc in which the spin of the Be star is misaligned with the orbital axis of a neutron star companion. Tidal torques from the neutron star truncate the disc at a radius small enough that the neutron star orbit does not intersect the disc unless the eccentricity or misalignment is very large. A magnetic torque from the Be star that is largest at the equator, where the rotation is fastest, is approximated by an inner boundary condition. There are large oscillations in the mass and inclination of the disc as it moves towards a steady state. These large variations may explain the observed changes from Be star to Be shell star and vice-versa and also the Type II X-ray outbursts. We find the tidal timescale on which the disc warps, precesses and reaches a steady state to be around a year up to a few hundred years. If present, the oscillations in mass and disc inclination occur on a fraction of this timescale depending on the orbital parameters of the binary. The timescales associated with the tidal torque for observed Be star binaries suggest that these effects are important in all but the longest period binaries.

Key words:

accretion, accretion discs– binaries: general – stars: emission line, Be

1 INTRODUCTION

Be stars are rapidly rotating close to their break up velocity (Porter 1996). They are early type main-sequence stars which have shown H α in emission at least once. They are variable in brightness and spectra which show broad HeI absorption and emission at either visual or UV wavelengths. It is found that the emission, and so presumably their discs, are only temporary and so Be stars become B stars and vice versa. Be star discs form and disappear on a timescale of a few months to a few years (Telting et al. 1998; Bjorkman 2000, 2002). More recently, Rajoelimanana, Charles & Udalski (2010) observed the optical emission from Be X-ray binaries in the SMC and found superorbital quasi-periodic variations on timescales of about 200 – 3000 d that are thought to be related to the formation and depletion of the circumstellar discs.

We choose to model the Be star disc as a viscous decretion disc. Several other models have previously been proposed to describe the physical structure of the disc such as

the wind-compressed disc model and the magnetically wind-compressed disc model (see Porter & Rivinius 2003, for a review). In the wind-compressed disc model the rotation of the star produces a wind towards the equator. The material from both sides collides at the equator and the shock produces a dense region confined to the equatorial plane by the opposing winds from each side (Bjorkman & Casinelli 1993). However, non-radial effects because of the rotation of the star ruled out this picture from dynamical arguments. It cannot reproduce the observed IR excess or kinematic structure (Porter 1997). An attempt to revive this model was made with the addition of magnetic fields (Cassinelli & MacGregor 2000). However, numerical simulations of this model still do not explain the observations when stellar rotation is included (Owocki & ud Doula 2003). The most likely alternative to the wind-compressed disc model is the viscous disc model that we have used in this work.

The disc is modelled as a viscous decretion discs with the mass expelled from the neighbourhood of the Be star itself (Lee, Saio & Osaki 1991; Cassinelli et al. 2002). Hanuschik (1996) finds that the discs are rotationally supported and Quirrenbach et al (1997) deduced that the circumstellar envelopes around Be stars

* E-mail: rmartin@stsci.edu

are thin discs from interferometry of H α emission. Wood, Bjorkman & Bjorkman (1997) showed that the discs have an opening angle of about 2.5° with polarimetry and this is consistent with a Keplerian disc. This is equivalent to an aspect ratio $H/R \approx 0.04$.

Decretion discs have a different structure to accretion discs because the inner boundary condition is different (Pringle 1991). In an accretion disc the inner boundary has zero torque and accretion is allowed on to the central object. In a decretion disc, the inner boundary prevents flow there on to the central object. The disc grows when the star exerts a positive torque on it or decays when there is no torque. If mass is injected on to an accretion disc, then outside of the injection radius, the disc is a decretion disc. Continual addition of angular momentum allows the viscosity to transport angular momentum outwards though the disc and the disc mass moves outwards. There are mathematical disc solutions for the surface density of decretion discs which either have infinite mass or divergent radial velocity (Okazaki 2007). There is a third steady state decretion disc solution where there is no flow either in or out. Flow may be prevented in the outer regions of a disc by a torque, such as tides from a companion star and in the inner regions by a magnetic torque from the central star.

If the disc is viewed edge on the Be star is seen as a shell star. Two Be stars, γ Cas and 59 Cyg have shown two successive shell events. which have been explained by a disc that is tilted with respect to the equatorial plane of the star (Hummel 1998). The variation in emission line widths and profile shapes are then due to the precession of the disc. The idea that a disc might change its inclination to the line of sight is further investigated through observations of 28 Tau (Pleione) by Hirata (2007). This star also changes between B star, Be star and shell star on a 35 yr timescale and the intrinsic polarization angle changes in phase with these variations. The cause of the precession is also not clear but Hummel (1998) suggested that it might be induced by tides from a binary companion as most Be stars have a neutron star companion.

Be/X-ray binaries show three types of X-ray activity (Stella, White & Rosner 1986; Negueruela et al. 1998). Type I outbursts are the periodic X-ray outbursts that coincide with periastron passage with a luminosity $L_X = 10^{36} - 10^{37} \text{ erg s}^{-1}$. Type II outbursts last weeks to months and show no orbital modulation but have a larger luminosity of $L_X > 10^{37} \text{ erg s}^{-1}$. It has been suggested that the Type II outbursts are linked to the interaction of the fast stellar wind with a warped disc (Negueruela et al. 2001; Okazaki 2001). The third type of X-ray activity is persistent low luminosity X-ray emission with $L_X < 10^{34} \text{ erg s}^{-1}$. In this work we consider the warping and precession of Be star discs with a neutron star companion on an orbit that is misaligned with the spin of the Be star and attempt to explain this activity.

In Section 2 we consider general properties of accretion and decretion disc structure. In Section 3 we consider properties of a decretion disc model warped by a tidal torque and in Section 4 we make numerical models. In Section 5 we apply the models to observed Be and B star binaries and consider how they are affected by a tidal torque.

2 DISC STRUCTURE

We model the structure and evolution of warped accretion discs according to the simplified formalism described by Pringle (1992). We consider the disc to be made up of annuli of width dR and mass $2\pi\Sigma R dR$ at radius R from the central Be star of mass M_1 with surface density $\Sigma(R, t)$ at time t . The material is in Keplerian orbits with angular velocity $\Omega = \sqrt{GM_1/R^3}$. The angular momentum at radius R is

$$\mathbf{L} = (GM_1 R)^{1/2} \Sigma \mathbf{l} = L \mathbf{l}, \quad (1)$$

where $\mathbf{l} = (l_x, l_y, l_z)$ is a unit vector describing the direction of the angular momentum of a disc annulus with $|\mathbf{l}| = 1$.

We use equation (2.8) of Pringle (1992) and add the binary tidal torque, \mathbf{T}_{tid} , and the angular momentum source term, $\dot{\mathbf{L}}_{\text{acc}}$, to give

$$\begin{aligned} \frac{\partial \mathbf{L}}{\partial t} = & \frac{1}{R} \frac{\partial}{\partial R} \left[\left(\frac{3R}{L} \frac{\partial}{\partial R} (\nu_1 L) - \frac{3}{2} \nu_1 \right) \mathbf{L} + \frac{1}{2} \nu_2 R L \frac{\partial \mathbf{l}}{\partial R} \right] \\ & + \frac{1}{R} \frac{\partial}{\partial R} \left(\nu_2 R^2 \left| \frac{\partial \mathbf{l}}{\partial R} \right|^2 \mathbf{L} \right) + \mathbf{T}_{\text{tid}} + \dot{\mathbf{L}}_{\text{acc}}. \end{aligned} \quad (2)$$

The source of angular momentum by mass accretion on to the disc from the Be star is

$$\dot{\mathbf{L}}_{\text{acc}} = \frac{\dot{M}}{2\pi R_{\text{add}}} R_{\text{add}}^2 \Omega_{\text{add}} \delta(R - R_{\text{add}}) \mathbf{j}_{\text{Be}}, \quad (3)$$

where

$$\mathbf{j}_{\text{Be}} = (\sin \theta, 0, \cos \theta) \quad (4)$$

is the direction of the spin of the Be star. We assume the material added has angular momentum aligned with the Be star spin and it is injected at a radius R_{add} so that $\Omega_{\text{add}} = \Omega(R_{\text{add}})$. We work in the frame where the binary orbital axis is $(0, 0, 1)$. We discuss the tidal torque in Section 3.

There are two viscosities. First ν_1 corresponds to the azimuthal shear, the viscosity normally associated with accretion discs, and secondly ν_2 corresponds to the vertical shear in the disc which smooths out the twist. The second viscosity acts when the disc is non-planar. With the α -parametrisation the viscosities are given by

$$\nu_i = \alpha_i c_s H \quad (5)$$

(Shakura & Sunyaev 1973), where $i = 1, 2$, $c_s = H\Omega$ is the sound speed and H is the scale height of the disc. The dimensionless parameters $\alpha_1 \leq 1$ and α_2 must be determined experimentally. Lee, Saio & Osaki (1991) suggest that with $\alpha = 0.1$ it will take too long for the disc mass to build up so we choose $\alpha_1 = 0.3$ (e.g. Jones, Sigut & Porter 2008). Ogilvie (1999) found the viscosities to be related by

$$\frac{\nu_2}{\nu_1} = \frac{\alpha_2}{\alpha_1} = \frac{1}{2\alpha_1^2} \frac{4(1 + 7\alpha_1^2)}{4 + \alpha_1^2} \quad (6)$$

and more recently Lodato & Price (2010) have verified this numerically. With $\alpha_1 = 0.3$ then we find the corresponding $\alpha_2 = 2.66$. We note that varying α affects only the timescales of the effects discussed in this work.

2.1 Steady State Discs

In this section let us consider steady state discs. We set $\partial \mathbf{L} / \partial t = 0$ then take the scalar product of equation (2)

with \mathbf{l} to find

$$0 = \frac{1}{R} \frac{\partial}{\partial R} \left[3R \frac{\partial}{\partial R} (\nu_1 L) - \frac{3}{2} \nu_1 L \right] \quad (7)$$

because $\mathbf{T}_{\text{tid}} \cdot \mathbf{l} = 0$ (see Section 3.1). The tidal torque is zero when it acts in the same direction as the angular momentum of the disc at that radius. Equation (7) has the solution

$$\nu_1 \Sigma = A + BR^{-\frac{1}{2}}, \quad (8)$$

where A and B are constants to be determined by the boundary conditions. The first term is the accretion disc term for which $\nu_1 \Sigma = \text{const}$ (far from the inner radius) and the second term is the steady state decretion disc term which has $\nu_1 \Sigma \propto R^{-\frac{1}{2}}$ (Pringle 1991) and zero mass accretion rate through the disc.

The mass transfer rate through the disc is

$$\dot{M} = 2\pi R \Sigma (-v_R), \quad (9)$$

where the radial velocity in the disc is

$$v_R = -\frac{3}{\Sigma R^{\frac{1}{2}}} \frac{\partial}{\partial R} \left(\nu_1 \Sigma R^{\frac{1}{2}} \right) - \nu_2 R \left| \frac{\partial \mathbf{l}}{\partial R} \right|^2 \quad (10)$$

(Pringle 1981). The accretion rate is defined so that $\dot{M} > 0$ implies accretion, the material moves inwards, and $\dot{M} < 0$ implies decretion, the material moves outwards. The general steady state surface density in a disc is

$$\nu \Sigma = \frac{\dot{M}}{3\pi} \left[1 - \left(\frac{R_\star}{R} \right)^{\frac{1}{2}} \right] + \nu_{1\star} \Sigma_\star \left(\frac{R_\star}{R} \right)^{\frac{1}{2}}, \quad (11)$$

where Σ_\star and ν_\star are the surface density and viscosity at $R = R_\star$ and the steady rate of mass transfer through the disc is \dot{M} . The first term is the normal accretion disc term with $\nu \Sigma = 0$ at $R = R_\star$ and so zero torque at the inner boundary. The second term satisfies $v_R = 0$ when $\partial \mathbf{l} / \partial R$ is zero there. With the additional second term, we can vary the mass of the disc and the accretion rate through the disc independently even with a steady state disc. For a Be star disc that is truncated by the tides of a neutron star companion we take only the second term, the steady state decretion disc term (see Section 2.4 for more on the truncation of the disc).

2.2 Surface Density

The density of the disc is

$$\rho(R, z) = \rho_0 \left(\frac{R_\star}{R} \right)^n e^{-\left(\frac{z-z_0}{H} \right)^2}, \quad (12)$$

where z_0 is the height of the disc about the equatorial plane and is a function of radius, R . For a flat disc $z_0(R) = 0$ everywhere. By integrating the density over the disc height, z , we find the surface density of the disc to be

$$\Sigma = \int_{-\infty}^{\infty} \rho dz = \Sigma_\star \left(\frac{R_\star}{R} \right)^{n-\frac{3}{2}}, \quad (13)$$

with the constant

$$\Sigma_\star = \rho_0 \sqrt{\pi} H_\star. \quad (14)$$

Wood, Bjorkman & Bjorkman (1997) find that at the stellar radius the disc aspect ratio is $H_\star/R_\star \approx 0.04$. We choose a

typical density of $\rho_0 = 10^{-11} \text{ g cm}^{-3}$ and $n = 7/2$ and we find

$$\frac{\Sigma_\star}{\text{g/cm}^2} = 0.49 \left(\frac{H_\star/R_\star}{0.04} \right) \left(\frac{R_\star}{10 R_\odot} \right) \left(\frac{\rho_0}{10^{-11} \text{ g cm}^{-2}} \right). \quad (15)$$

We justify the choice of n through the viscosity.

2.3 Viscosity

For an isothermal disc the sound speed $c_s = \text{const}$ and so the disc scale height is $H = c_s/\Omega \propto R^{\frac{3}{2}}$. We use the α -prescription for the viscosities as in equation (5) and find

$$\nu_i = \alpha_i \left(\frac{H}{R^{\frac{3}{2}}} \right)^2 (GM_1)^{\frac{1}{2}} R^{\frac{3}{2}}, \quad (16)$$

where $i = 1, 2$. With equation (8) we have $\nu_1 \Sigma \propto R^{-\frac{1}{2}}$ in a steady state decretion disc and with (13) we found $\Sigma \propto R^{-n+\frac{3}{2}}$. The viscosity must therefore be parametrised as

$$\nu_i = \nu_{i\star} \left(\frac{R}{R_\star} \right)^{n-2}. \quad (17)$$

However, because $\nu_i \propto R^{\frac{3}{2}}$ with the α -prescription, for a consistent model we must choose $n = 7/2$. We find the viscosities at the stellar radius to be

$$\begin{aligned} \nu_{i\star} &= 1.69 \times 10^{17} \left(\frac{\alpha_i}{2.66} \right) \left(\frac{H_\star/R_\star}{0.04} \right)^2 \\ &\times \left(\frac{M_1}{17 M_\odot} \right)^{\frac{1}{2}} \left(\frac{R_\star}{10 R_\odot} \right)^{\frac{1}{2}} \text{ cm}^2 \text{ s}^{-1} \end{aligned} \quad (18)$$

for $i = 1, 2$. We note that if the disc was not isothermal, then we would change the radius power law for the scale height, H , of the disc. The value of n decreases so that the surface density would fall off more slowly with radius. This does not affect the shape of the warped disc in the numerical models in Section 4, only the scale height and surface density of the disc. Porter (2003) found that with a smaller value of n he was able to better reproduce the observed continuum emission.

The first viscous timescale describes the timescale over which mass flows through the disc and the second viscous timescale describes the how the disc smoothes out the warp and twist. The viscous timescales in the disc are

$$t_{\nu_i} = \frac{R^2}{\nu_i} = \frac{R_\star^2}{\nu_{i\star}} \left(\frac{R}{R_\star} \right)^{\frac{1}{2}} \quad (19)$$

and so we find

$$\begin{aligned} t_{\nu_i} &= 33.2 \left(\frac{\alpha_i}{2.66} \right)^{-1} \left(\frac{R_\star}{10 R_\odot} \right)^{\frac{3}{2}} \left(\frac{M_1}{17 M_\odot} \right)^{-\frac{1}{2}} \\ &\times \left(\frac{H_\star/R_\star}{0.04} \right)^{-2} \left(\frac{R}{R_\star} \right)^{\frac{1}{2}} \text{ d} \end{aligned} \quad (20)$$

for $i = 1, 2$. The viscous timescales increase with radius in the disc. For example, the minimum timescales at the inner edge of the disc at the stellar radius are $t_{\nu_1} = 294 \text{ d}$ and $t_{\nu_2} = 33.2 \text{ d}$. An accretion disc reaches steady state on the first viscous timescale. The disc smoothes out on the second viscous timescale.

2.4 Tidal Truncation of the Disc

Providing that the orbital period is shorter than the viscous timescale, $t_{\nu 1}$, in the outer parts of the disc then the tidal torques from the companion neutron star can truncate the disc. In the circular orbit case, the tidal truncation radius, R_t , can be estimated as where ballistic orbits begin to cross (Paczynski 1977). For example, in Figure 6 of Martin, Tout & Pringle (2008) this radius is shown as a function of mass ratio of the binary. For Be star systems, the mass ratio is in the approximate range $M_2/M_1 = 0.1-0.5$ so the truncation radius is $R_t \lesssim 0.5a$, where a is the semi-major axis of the orbit. In the eccentric binary case, the disc radius can be estimated by considering the effects of tidal resonances. As the eccentricity of the binary increases, the truncation radius of the disc decreases (Artymowicz & Lubow 1994). The neutron star orbit will be larger than the outer radius of the disc unless the eccentricity is close to 1 or there is a large misalignment angle.

We note that this has implications for theories of Type II X-ray outbursts. It has previously been suggested that they occur when the Be star disc becomes sufficiently large that the neutron star passes through the decretion disc. This is only possible if the disc does not become truncated fast enough which may happen if the eccentricity is close to 1 or if the misalignment angle is large enough that the truncation is not efficient. Okazaki (2007) suggested that the truncation becomes inefficient for large misalignments $\theta > 60^\circ$. In this work we consider smaller misalignments and note that observed misalignments of Be X-ray binaries are relatively small (e.g. Martin, Tout & Pringle 2009).

3 TIDAL WARPING

It is widely suggested that the warp and precession observed in Be star discs may be caused by a misalignment between the spin axis of the Be star and the orbit of the binary companion. Here we consider further the tidal torque.

3.1 Tidal Torque

The tidal torque in the frame of the binary orbit, of radius R_b , is approximately

$$\mathbf{T}_{\text{tid}} = -\frac{GM_2 R \Sigma}{2R_b^2} \left[b_{3/2}^{(1)} \left(\frac{R}{R_b} \right) \right] (\mathbf{e}_z \cdot \mathbf{l})(\mathbf{e}_z \times \mathbf{l}) \quad (21)$$

(Lubow & Ogilvie 2000; Ogilvie & Dubus 2001) to first order in the angle of tilt between the disc and the orbital plane. Here \mathbf{e}_z is a unit vector in the direction of the binary orbital axis, M_2 is the mass of the binary companion star and R_b is the binary separation. This tidal torque is averaged over a binary orbit. The Laplace coefficient of celestial mechanics can be approximated for small z by

$$b_{3/2}^{(1)}(z) = \frac{3}{2}z \left[1 + \frac{15}{8}z^2 + \frac{175}{64}z^4 + \dots \right]. \quad (22)$$

We note that it does indeed satisfy $\mathbf{l} \cdot \mathbf{T}_{\text{tid}} = 0$ (see Section 2) so that the tidal torque is zero when the disc and orbit are aligned. Thus even for large tilt angles the tidal torque term is likely to have this form, although with modified coefficients.

3.2 Orbital Parameters

Most Be star binaries have eccentric orbits and so the tidal torque will not be constant over an orbit. In an eccentric orbit, the stars spend a short time close to periastron but here, the torque will be stronger than in a circular orbit. Because the orbital period of the system is much smaller than the timescale on which the tidal torque acts (see Section 5) we can average the torque over an orbit. In this Section we find, for the average torque over an eccentric orbit, the equivalent average binary separation.

With Kepler's third law the binary semi-major axis is

$$a = \left(\frac{GM P^2}{4\pi^2} \right)^{\frac{1}{3}}, \quad (23)$$

where P is the orbital period and $M = M_1 + M_2$ and so

$$a = 6.50 \times 10^{12} \left(\frac{M}{18.4 M_\odot} \right)^{\frac{1}{3}} \left(\frac{P}{24.3 \text{ d}} \right)^{\frac{2}{3}} \text{ cm}. \quad (24)$$

From Kepler's first law, the separation of the binary stars in an eccentric orbit satisfies

$$R_b = \frac{a(1 - e^2)}{1 + e \cos \phi}, \quad (25)$$

where e is the eccentricity of the orbit and ϕ is the azimuthal angle around the orbit. With Kepler's second law

$$\frac{d}{dt} \left(\frac{1}{2} R_b^2 \dot{\phi} \right) = 0, \quad (26)$$

where $\dot{\phi} = d\phi/dt$. We integrate this equation twice over an orbit to find

$$\frac{1}{2} R_b^2 \dot{\phi} = \frac{\pi a^2}{P} (1 - e^2)^{\frac{1}{2}}. \quad (27)$$

The tidal torque found by Ogilvie & Dubus (2001) in equation (21) has a factor of $1/R_b^3$ which we must replace with its average in time

$$\begin{aligned} \left\langle \frac{1}{R_b^3} \right\rangle &= \frac{1}{P} \int_0^P \frac{1}{R_b^3} dt \\ &= \frac{1}{a^3 (1 - e^2)^{\frac{3}{2}}}. \end{aligned} \quad (28)$$

The average separation is thus

$$\bar{R}_b = a(1 - e^2)^{\frac{1}{2}} \quad (29)$$

(see e.g. Holman, Touma & Tremaine 1997). In Section 5 we find the tidal timescale for observed Be star binaries and there we must use equation (21) replacing R_b with \bar{R}_b so that we do not underestimate the strength of the tidal torque in an eccentric system.

3.3 Tidal Warp Radius

The tidal torque balances the viscous torque in the disc at the tidal warp radius. Outside of the tidal warp radius the disc is dominated by the tidal torque and inside of this radius by the viscous torques. The tidal warp radius is

$$R_{\text{tid}} = \left[\frac{2\nu_{2*} (GM_1)^{\frac{1}{2}} \bar{R}_b^3}{3GM_2 R_*^{n-2}} \right]^{\frac{2}{11-2n}} \quad (30)$$

(Martin, Pringle & Tout 2007, 2009). Note that in deriving this radius, only the first term in the expansion in equation (22) has been used. This is the same radius for accretion and decretion discs which have only a tidal torque because it is independent of surface density. We expect that well outside this radius the binary torque term, coupled with the viscosity, flattens the disc and it aligns with the binary orbital plane. If the disc does not extend up to the tidal radius, the torque can still have an effect on the disc and cause the disc to move towards alignment with the binary orbit even if they don't completely align.

With the standard parameters used in the previous Section we find with $n = 7/2$ that

$$R_{\text{tid}} = 3.68 \times 10^{12} (1 - e^2)^{\frac{3}{4}} \left(\frac{P}{24.3 \text{ d}} \right) \left(\frac{\alpha_2}{2.66} \right)^{\frac{1}{2}} \\ \times \left(\frac{M_1}{17 M_{\odot}} \right)^{\frac{1}{2}} \left(\frac{M_2}{1.4 M_{\odot}} \right)^{-\frac{1}{2}} \left(\frac{M}{18.4 M_{\odot}} \right)^{\frac{1}{2}} \\ \times \left(\frac{R_{\star}}{10 R_{\odot}} \right)^{-\frac{1}{2}} \left(\frac{H_{\star}/R_{\star}}{0.04} \right) \text{ cm}. \quad (31)$$

If $n = 4$ (as we have used for our numerical models in Section 4) then we find $R_{\text{tid}} = 6.1 \times 10^{12} \text{ cm}$ for these general parameters. With the small orbital period shown here the warp radius is within the disc. However for Be star systems of longer period, it may be outside of the disc. In this case the viscous torques in the disc always dominate the tidal torques. The disc is relatively flat, but may be tilted from the equator of the Be star and precessing.

3.4 Tidal Timescale

The timescale on which the tidal torque acts is equal to the viscous timescale at $R = R_{\text{tid}}$ by definition. It scales as

$$t_{\text{tid}} = \frac{R_{\star}^2}{\nu_{2\star}} \left(\frac{R_{\text{tid}}}{R} \right)^{\frac{3}{2}}. \quad (32)$$

We parametrise this as

$$t_{\text{tid}} = t_{\text{tid}\star} \left(\frac{R}{R_{\star}} \right)^{-\frac{3}{2}}, \quad (33)$$

where the tidal timescale at $R = R_{\star}$ is

$$t_{\text{tid}\star} = 1.1 (1 - e^2)^{\frac{9}{8}} \left(\frac{P}{24.3 \text{ d}} \right)^{\frac{3}{2}} \left(\frac{\alpha_2}{2.66} \right)^{-\frac{1}{4}} \\ \times \left(\frac{M_1}{17 M_{\odot}} \right)^{\frac{1}{4}} \left(\frac{M_2}{1.4 M_{\odot}} \right)^{-\frac{3}{4}} \left(\frac{M}{18.4 M_{\odot}} \right)^{\frac{3}{4}} \\ \times \left(\frac{R_{\star}}{10 R_{\odot}} \right)^{-\frac{3}{4}} \left(\frac{H_{\star}/R_{\star}}{0.04} \right)^{-\frac{1}{2}} \text{ yr}. \quad (34)$$

The disc aligns with the binary orbital plane on this timescale. This is longer than the orbital period and so the disc inclination should eventually reach a steady state.

4 EVOLUTION OF THE MISALIGNED DISC

We solve equation (2) numerically with a first order explicit method (Pringle 1992) including the non-linear terms. We concentrate on the effects of the tidal torque, without which the disc would remain flat and aligned with the spin axis

of the Be star. The size of Be star discs has been observed in a few cases. Grundstrom & Gies (2006) used results from a H α monitoring campaign to find the Be stars that they considered had discs with an outer edge in the range 3 – 11 R_{\star} . In this work we choose the Be star to have an outer truncation radius of $R_{\text{out}} = 10 R_{\star}$. We use 200 grid points distributed logarithmically between the inner radius $R_{\text{in}} = R_{\star}$ and the outer radius R_{out} .

The inclination of the disc angular momentum to the binary orbital axis is

$$i(R) = \cos^{-1}(l_z) \quad (35)$$

and the azimuthal angle is

$$\omega(R) = \tan^{-1} \left(\frac{l_y}{l_x} \right). \quad (36)$$

The tidal precession can be parametrised as

$$\mathbf{T}_{\text{tid}} = \boldsymbol{\Omega}_{\text{tid}} \times \mathbf{L} \quad (37)$$

(see Martin, Pringle & Tout 2009), where we choose coordinates so that

$$\boldsymbol{\Omega}_{\text{tid}} = \frac{1}{t_{\nu_2}(R_{\text{tid}})} \left(\frac{R}{R_{\text{tid}}} \right)^{\frac{3}{2}} \mathbf{e}_z. \quad (38)$$

This term has the effect of precessing the disc about the \mathbf{e}_z axis when the disc is not aligned with the binary orbital plane. This corresponds to the first term in the expansion given in equation (22).

Initially the disc has very little mass that is flat and aligned with the spin of the Be star as given in equation (4), where θ is the misalignment between the spin of the Be star and the binary orbital axis. Mass is injected on to the disc at a constant rate \dot{M} at a radius of $R_{\text{add}} = 1.1 R_{\star}$. The mass is always added with an angular momentum aligned with the spin axis of the Be star which in all models is misaligned to the binary orbital axis by $\theta = 25^\circ$.

We need three boundary conditions at the inner and outer edges of the disc. We choose two conditions on the direction of the angular momentum at both edges, $\partial \mathbf{l} / \partial R = 0$ with $|\mathbf{l}| = 1$. We need one more condition on the surface density. In this work we consider three different surface density inner boundary conditions that we describe in the Section 4.1. We use a zero radial velocity surface density outer boundary condition, $v_R = 0$, at R_{out} because we assume that the outer radius is truncated by the tidal torque from the neutron star. Tidal torques truncate the edge of a disc over a small radius (e.g. Ichikawa & Osaki 1994; Martin & Lubow 2011). Okazaki (2002) use a 3D SPH code to model a Be star disc that is coplanar with the neutron star orbit. They find that the disc is truncated if $\alpha_1 \ll 1$. With the neutron star companion, the disc becomes denser than the disc around an isolated Be star. Okazaki & Hayasaki (2007) extend this model to a disc that is inclined to the binary orbital plane. They have material accreted on to the Be star disc for 50 orbital periods and then they turn off the accretion. They find that there is little precession until the accretion is turned off. With a one-dimensional code we can evolve the disc for a longer period of time.

We choose the first viscosity

$$\nu_1 = 0.1 \left(\frac{R}{R_{\star}} \right)^2 R_{\star}^2 t_c^{-1} \quad (39)$$

and the second viscosity

$$\nu_2 = \left(\frac{R}{R_*}\right)^2 R_*^2 t_c^{-1}, \quad (40)$$

where we have defined the time unit

$$t_c = t_{\nu_2}(R_*), \quad (41)$$

which with equation (20) for our standard parameters $t_{\nu_2} = 58.8$ d. With these viscosities the viscous timescales are constant in radius through the disc and the evolution proceeds at the same rate at all radii. This is slightly different from the prescription we found in Section 2.

4.1 Inner Boundary Condition

The inner boundary condition is an approximation to a torque applied close to the star that depends on the magnetic field of the Be star. We assume that the magnetic axis is aligned with the spin of the Be star. We first consider a torque that is strong enough to prevent all accretion back on to the Be star. This is equivalent to $v_R = 0$ at R_* or else

$$\left. \frac{\partial}{\partial R} (\nu_1 \Sigma R^{\frac{1}{2}}) \right|_{R=R_*} = 0 \quad (42)$$

(Pringle 1991). Next we consider a disc with no additional torque from the star so that the inner boundary condition is $\Sigma = 0$ at $R = R_*$ (Pringle 1981). Finally we choose a magnetic torque that varies with the inclination of the inner edge of the disc. The torque is strongest when the disc is aligned with the equator of the star but weakens as the inner disc moves away from the equator. We parametrise the inner boundary condition with

$$\left. \frac{\partial}{\partial R} (\nu_1 \Sigma R^{\frac{1}{2}}) \right|_{R=R_*} = K \frac{\nu_{1*} \Sigma_*}{R_*^{\frac{1}{2}}} \left[\frac{\Omega_*/\Omega_{\text{star}}}{\cos(i_* - \theta)} - 1 \right], \quad (43)$$

where $\Omega_* = \Omega(R_*)$, $i_* = i(R_*)$, Ω_{star} is the angular velocity of the Be star and K is a constant we can vary. We note that the zero radial velocity and zero surface density inner boundary conditions represent the two limiting cases of possible inner boundary conditions. We consider all these boundary conditions further in the Appendix and show that the evolution is the same with an extra torque term acting on the disc.

4.2 Zero Radial Velocity Inner Boundary

The zero radial velocity inner boundary condition is given in equation (42). In this case flow is prevented from both the inner and outer edge of the disc and so there is no mass loss from the disc. Mass is added to the disc at a constant rate and so the mass of the disc increases linearly in time

$$M_d = \left(\frac{t}{t_c}\right) \dot{M} t_c. \quad (44)$$

For example if the mass accretion rate on to the disc is $\dot{M} = 10^{-9} M_\odot \text{ yr}^{-1}$ and the second viscous timescale at the inner edge of the disc is $t_{\nu_2}(R_*) = 58.8$ d = t_c . At a time of $t = 243 t_c$ the mass of the disc would be $M_d = 3.9 \times 10^{-8} M_\odot$.

In Fig 1 we show the inclination and azimuthal angle of the angular momentum vector and the surface density of such a disc which has a binary companion misaligned

by $\theta = 25^\circ$ and a tidal warp radius of $R_{\text{tid}} = 5 R_*$. Mass is injected at R_{add} and initially the mass moves outwards. Once it reaches the outer boundary where the disc becomes truncated it reaches a steady state where there is no flow in the disc. The surface density continues to increase steadily in time once it has reached its steady state of $\nu \Sigma \propto R^{-\frac{1}{2}}$ (Pringle 1991). The tidal torque is strongest at the outside of the disc and so initially the outer parts of the disc align with the binary orbital axis and the inner parts follow. The tidal timescale at the inner radius is $t_{\text{tid}}(R_*) = 11.1 t_c$ (with equation 32). At this time, the disc has become significantly misaligned with the spin of the Be star (left hand plot) and significantly twisted (middle plot). The surface density has reached its quasi steady state. The tidal timescale at the outer radius in the disc is $t_{\text{tid}}(10 R_*) = 0.35 t_c$. At this time, the disc is still close to alignment with the equator of the Be star.

In Fig. 2 we consider a disc with a larger tidal warp radius of $R_{\text{tid}} = 20 R_*$. This is outside of the outer edge of the disc. The viscous torques in the disc are always larger than the tidal torques. The surface density evolution is the same as in Fig. 1 because it is independent of the tidal warp radius. The disc is less warped and twisted with a larger tidal warp radius. It moves more like a solid body. The tidal timescale at the inner edge of the disc is $t_{\text{tid}}(R_*) = 89.4 t_c$. At this time the disc has moved significantly from the initial alignment with the Be star equator. In the bottom right hand plot we show the evolution of the angular momentum vectors at the inner and outer edge of the disc in time. Initially the disc has $l_y = 0$ and both vectors are the same, on the right hand side of the plot. The disc precesses about the binary orbital axis at the origin.

From the two figures in this Section we conclude that the Be star disc aligns and precesses with the binary orbital plane on the tidal timescale at the inner edge of the disc. Once the disc mass is large enough, the additional torque on the disc from the injected matter becomes small compared with the torque from the binary companion in the larger mass disc so the disc always becomes aligned with the plane of the binary orbital axis, no matter what the warp radius is.

4.3 Zero Torque Inner Boundary Condition

The second inner boundary condition that we consider is a zero torque inner boundary condition normally associated with accretion discs

$$\Sigma(R_*) = \Sigma_* = 0. \quad (45)$$

As before material is continuously injected at R_{add} and it moves both outwards and inwards. In $R > R_{\text{add}}$ the disc behaves as a decretion disc and in $R < R_{\text{add}}$ as a normal accretion disc.

In Fig. 3 we plot the evolution of a system with $R_{\text{tid}} = 5 R_*$. In this example the disc mass reaches a steady state of $M_d = 0.36 \dot{M} t_c$. Because the disc mass is lower than in the previous case, the mass addition torque is relatively stronger compared with the tidal torque and so the inner parts of the disc remain close to alignment with the Be star equator while the outer parts tend towards alignment with the binary orbital plane. We do not show the evolution of the angular momentum vector in this Section because there is very little

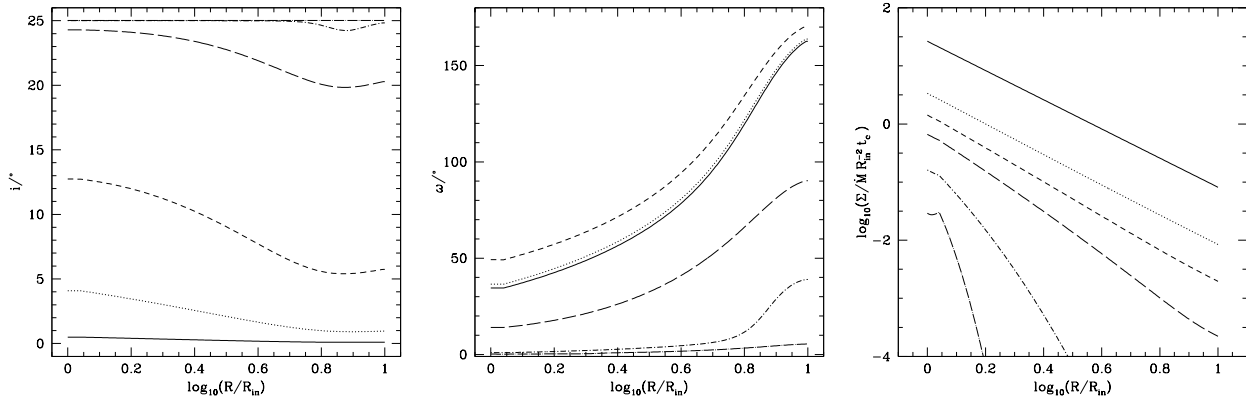


Figure 1. The disc has a warp radius of $R_{\text{tid}} = 5 R_*$ and a misalignment of $\theta = 25^\circ$. The inner boundary condition is $v_R = 0$. The evolution of the inclination of the disc angular momentum to the binary orbital axis (left), the azimuthal angle (middle) and the surface density (right) of the disc. The times shown are $t = 0.037$ (long dot dashed lines), 0.33 (short dot dashed lines), 3.0 (long dashed lines), 9.0 (short dashed lines), 27.0 (dotted lines) and $243 t_c$ (solid lines), where the time unit is defined in equation (41). The mass of the disc increases linearly in time.

precession with the zero torque angular momentum inner boundary condition.

4.4 Varying Radial Velocity at the Inner edge

In this Section we consider the inner boundary condition that varies with the inclination of the inner disc to the equator of the Be star given in equation (43). Unless otherwise stated we consider the Be star to be rotating at break up velocity so that $\Omega_{\text{star}} = \Omega_*$. In Fig. 4 we plot the inclination, azimuthal angle and surface density of a disc with a tidal warp radius of $R_{\text{tid}} = 5 R_*$ and $K = 100$. Once the inner edge of the disc moves away from the Be star equator, accretion on to the Be star begins. The disc reaches a steady state that similar to the one with the zero torque inner boundary condition (shown in Fig. 3) but now is closer to alignment with the binary plane because there is more mass in the disc.

In Fig. 5 we plot the evolution of the mass of the disc (left) and the inclination of the inner disc edge relative to the binary orbital plane (right) for discs with $R_{\text{tid}} = 5, 20$ and $80 R_*$ and $K = 10$. There is competition between the tidal torque, the mass addition torque and the magnetic torque which causes oscillations in the mass and inclination of the inner disc. Eventually the disc always reaches a warped and twisted steady state. The larger the tidal warp radius, the larger in both amplitude and number the oscillations are in mass and inner inclination of the disc. With a larger warp radius, the steady state mass of the disc is larger and the inclination of the inner disc is closer to the Be star equator. The discs shown in Fig. 5 have warp radii of $R_{\text{tid}} = 5, 20$ and $80 R_*$ so their corresponding tidal timescales at the inner edge are $11.1, 89.4$ and $715 t_c$. This is the timescale that the discs reach their steady state. The oscillations occur on a timescale shorter than this.

Once the disc mass has built up to a steady state, the only way for the oscillations to reoccur is for the disc mass to be lost or the accretion on to the disc to slow or cease. For example, if the driving mechanism behind the mass ejection from the star is pulsation then it is possible that the oscil-

lations will continue as the accretion on to the disc varies over time.

In Fig. 6 we consider the effect of varying the constant K . We plot the surface density and inclination of the inner parts of the disc, and the total disc mass with varying K for $R_{\text{tid}} = 20 R_*$. The larger K , the smaller the disc mass and surface density at the inner edge. The larger K , the larger the steady state inclination of the disc to the binary orbit. We also plot the evolution of the zero radial velocity inner boundary condition and see that when the tidal warp radius is outside of the disc then there are small oscillations in inclination of the disc as the disc approaches the binary orbital plane. Precession of the angular momentum vector is shown in the bottom right plot of Fig. 2 also.

In Fig. 7 we plot the evolution of the angular momentum vector at the inner and outer edge of the disc for a disc with $R_{\text{tid}} = 20 R_*$ and $K = 10$ which we can compare with the similar plot in Fig. 2 which instead had a zero radial velocity inner boundary condition. We see clearly the disc precesses about the steady state solution.

In all of the models shown so far, the viscosity radius power law index is $n = 4$ (see equation 17). However, Waters, Cote & Lamers (1987) and Dougherty et al. (1994) matched the infrared excess of a large sample of Be stars and found the index to be in the range $2 \leq n \leq 5$. An isothermal disc theoretically requires $n \geq 3.5$ for outflow (Porter 1999). More recently Jones, Sigut & Porter (2007) used hydrodynamical simulations of the disc structure and predicted the range $3 \leq n \leq 3.5$ in the inner regions of the disc. In Fig. 8 we show the effect of varying the viscosity parameters n and α_2/α_1 . Comparing the solid line (with $n = 4$), the long dashed line (with $n = 7/2$) and the dotted line (with $n = 3$), we find the smaller n is the longer the timescale of the oscillations. However, qualitatively the results are similar. We note that when we vary n , we change the viscous timescales. In order to compare models with the same tidal warp radius but varying n , the second viscous timescale at the inner edge of the disc changes as $t_c(n) = t_c(n = 4)(R_*/R_{\text{tid}})^{4-n}$. Comparing the long-dashed line ($\alpha_2/\alpha_1 = 0.1$) with the short-dashed line ($\alpha_2/\alpha_1 = 0.02$), we see that with a smaller

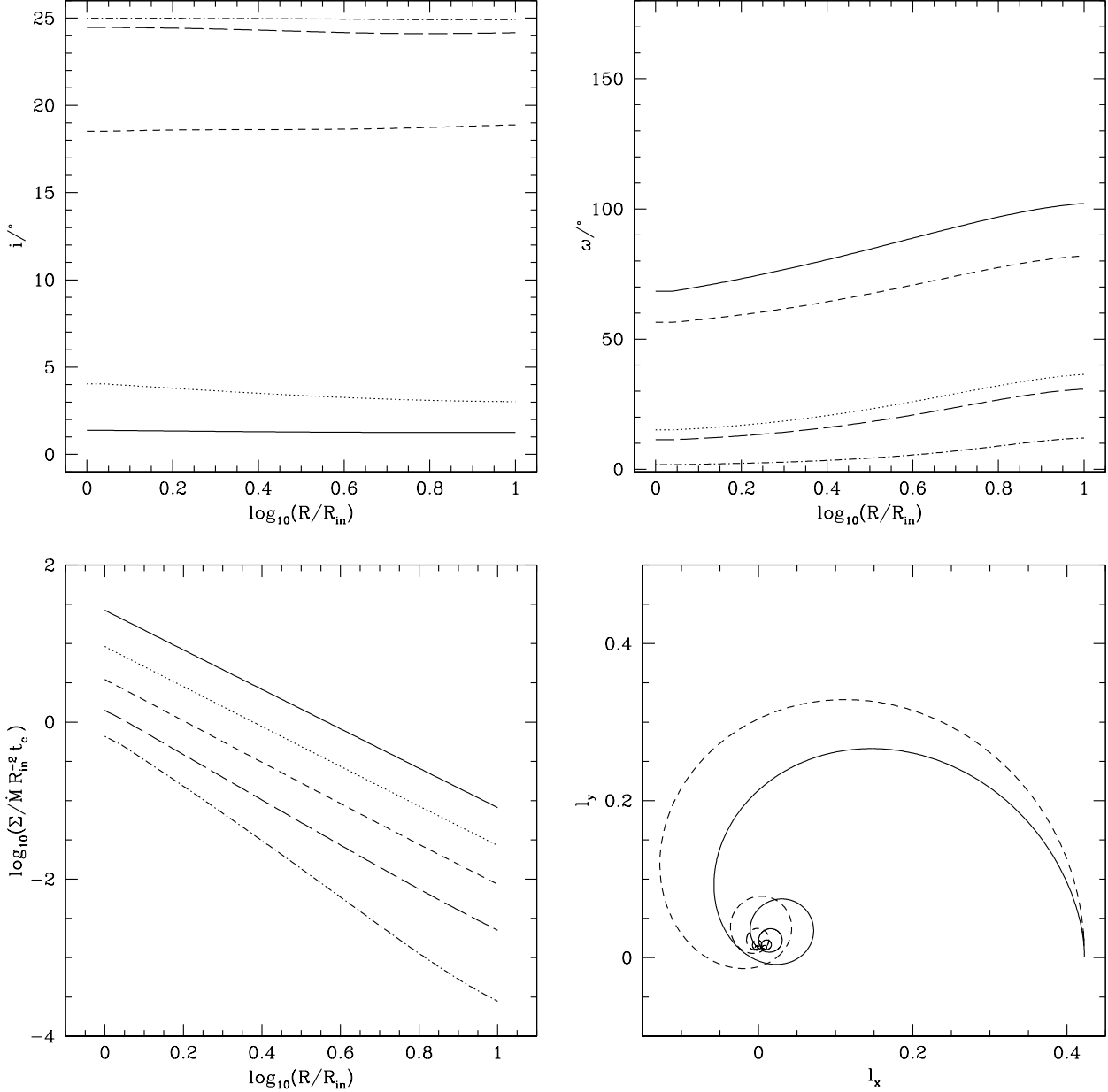


Figure 2. The zero radial velocity inner boundary condition for a disc with $R_{\text{tid}} = 20 R_\star$ and $\theta = 25^\circ$. The evolution of the inclination of the disc angular momentum to the binary orbital axis (top left), the azimuthal angle (top right) and the surface density (bottom left) of the disc in time. The times shown are $t = 3.0$ (dot-dashed lines), 9.0 (long dashed lines), 27.0 (short dashed lines) 81 (dotted lines) and $243 t_c$ (solid lines), where the time unit is defined in equation (41). The mass of the disc increases linearly in time. The bottom right plot shows the evolution of the angular momentum vector of the inner (solid line) and outer (dashed line) edges of the disc. At $t = 0$ the disc is at $l_y = 0$ on the right hand side of the plot.

value of α_2/α_1 the oscillations become slightly larger and the steady state is closer to alignment with the binary orbit. However, the qualitative behaviour of the system is similar with varying α_2/α_1 .

We have only considered Be stars that are rotating at break up with $\Omega_{\text{star}} = \Omega_\star$. We note that if $\Omega_{\text{star}} < \Omega_\star$ then the oscillation amplitude decreases and the disc moves to steady state more quickly.

5 OBSERVED BE STAR BINARIES

In Table 1 we show some Be and B star binaries that have been suggested to have a warped or tilted disc or have a measured misalignment between the Be star spin and the binary orbital axis. There is one B star binary because it has a measured misalignment and it is thought that B stars become Be stars and vice versa. We show the spectral type, the period, P , the eccentricity, e , and the measured inclination, θ , between the spin of the Be star and the axis of rotation

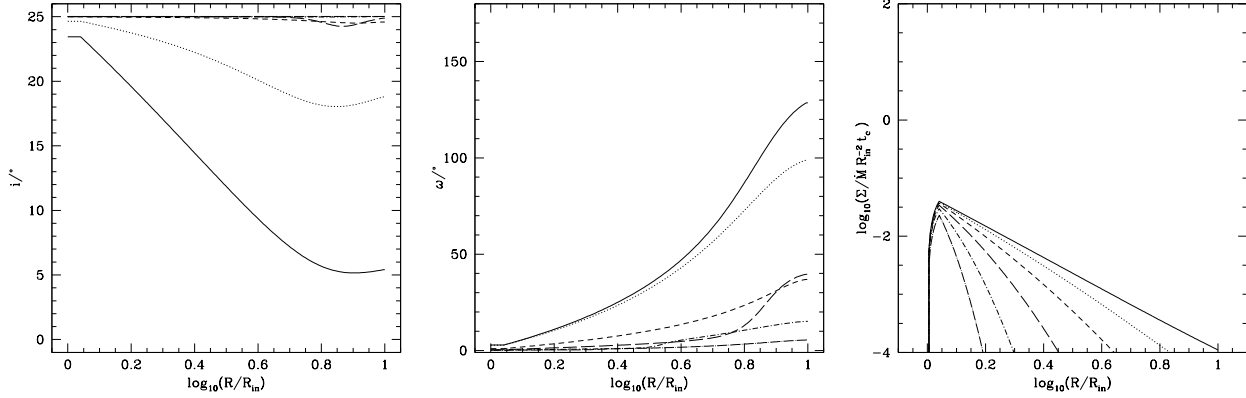


Figure 3. The inner boundary condition is $\Sigma_\star = 0$ for a disc with $R_{\text{tid}} = 5 R_\star$ and $\theta = 25^\circ$. The evolution of the inclination (left), azimuthal angle (middle) and surface density (right) of the disc in time. The times shown are $t = 0.037$ (long dot dashed lines), 0.11 (short dot dashed lines), 0.33 (long dashed lines), 1.0 (short dashed lines), 3.0 (dotted lines) and $81 t_c$ (solid lines). The time unit is defined in equation (41).

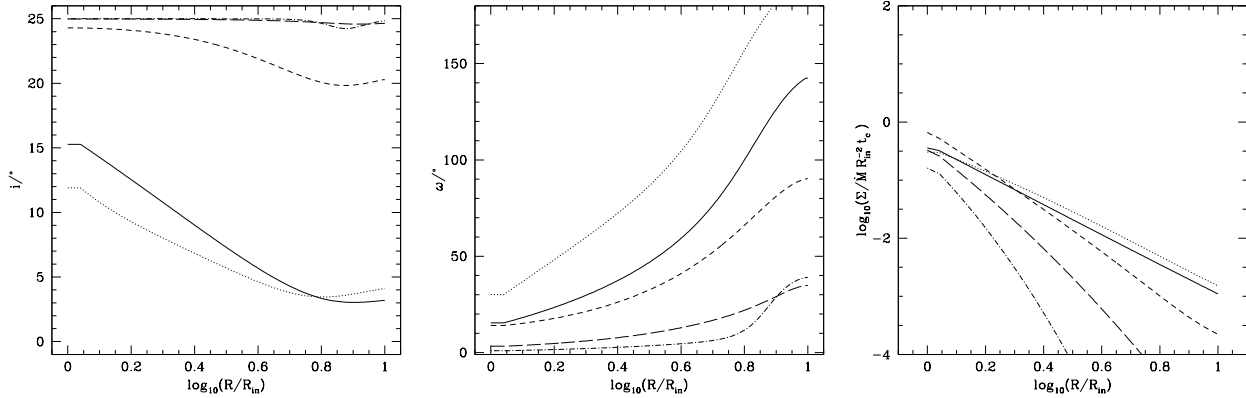


Figure 4. The inner boundary condition is the one given in equation (43) that varies with inclination of the inner disc to the Be star with $K = 100$. The disc has $R_{\text{tid}} = 5 R_\star$ and $\theta = 25^\circ$. The evolution of the inclination (left), azimuthal angle (middle) and surface density (right) of the disc at times $t = 0.33$ (dot dashed lines), 1.0 (long dashed lines), 3.0 (short dashed lines), 9.0 (dotted lines) and $27.0 t_c$ (solid lines) where the time unit is defined in equation (41).

| Be/B Star Binary | Spectral Type | P/d | e | $\theta/^\circ$ |
|--------------------------|---------------------------|---------------------|----------------------|--------------------------------|
| 4U0115+634 (V635 Cas) | B0.2 Ve | 24.3 | 0.34 ^[1] | unknown ^[2] |
| 59 Cyg | B1e ^[3] | 28.2 | 0.2 ^[4] | unknown ^[5] |
| J0045-7319 | B1 V | 51.2 | 0.808 ^[6] | 25 – 41 ^{[7],[8],[9]} |
| A0535+262 (V725 Tau) | B0 III-Ve ^[10] | 111 ^[11] | 0.47 ^[12] | unknown ^[13] |
| ζ Tau | B2 III | 133 ^[17] | | unknown ^[18] |
| 0053+604 (γ Cas) | B0.5 IVe | 203.59 | 0.26 ^[14] | ≈ 25 ^[5] |
| 28 Tau | B8e | 218 | 0.6 ^[15] | 59 ^[16] |
| SS 2883 (B1259-63) | B2e | 1236.7 | 0.87 ^[7] | > 55 ^{[7],[6]} |

Table 1. Binary Be stars and binary B stars that have either an observed misalignment or inferred warping. We show in column 3 the orbital period, P , column 4 the eccentricity, e and column 5 the misalignment, θ , between the spin of the Be star and the binary orbital axis. Where there is no measured misalignment we give references for the inferred warped, tilted or precessing disc. ^[1]Rappaport et al. (1978) ^[2]Negueruela et al. (2001) ^[3]Harmanec et al. (2002) ^[4]Rivinius & Štefl (2000) ^[5]Hummel (1998) ^[6]Wex et al. (1998) ^[7]Hughes (1999) ^[8]Kaspi et al. (1996) ^[9]Lai, Bildsten & Kaspi (1995) ^[10]Steele et al. (1998) ^[11]Hutchings (1984) ^[12]Negueruela et al. (2000) ^[13]Larionov, Lyuty & Zaitseva (2001) ^[14]Harmanec et al. (2000) ^[15]Katahira et al. (1996) ^[16]Hirata (2007) ^[17]Harmanec (1984) ^[18]Schaefer et al. (2010)

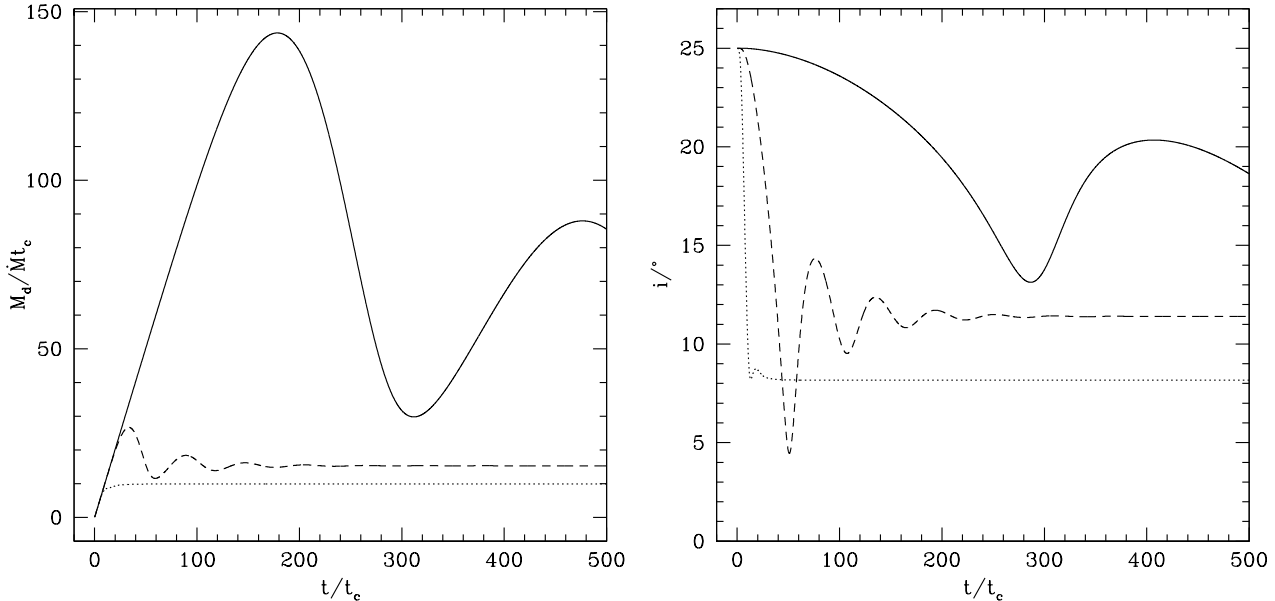


Figure 5. Three models with the varying inner boundary condition in equation (43) with $K = 10$. Left: The evolution of the total mass in the disc. Right: The evolution of the inclination of the inner edge of the disc. The spin of the Be star is at a misalignment of $\theta = 25^\circ$ in all three cases. The dotted lines show a model with $R_{\text{tid}} = 5 R_*$, the dashed lines with $R_{\text{tid}} = 20 R_*$ and the solid lines with $R_{\text{tid}} = 80 R_*$. The time unit is defined in equation (41).

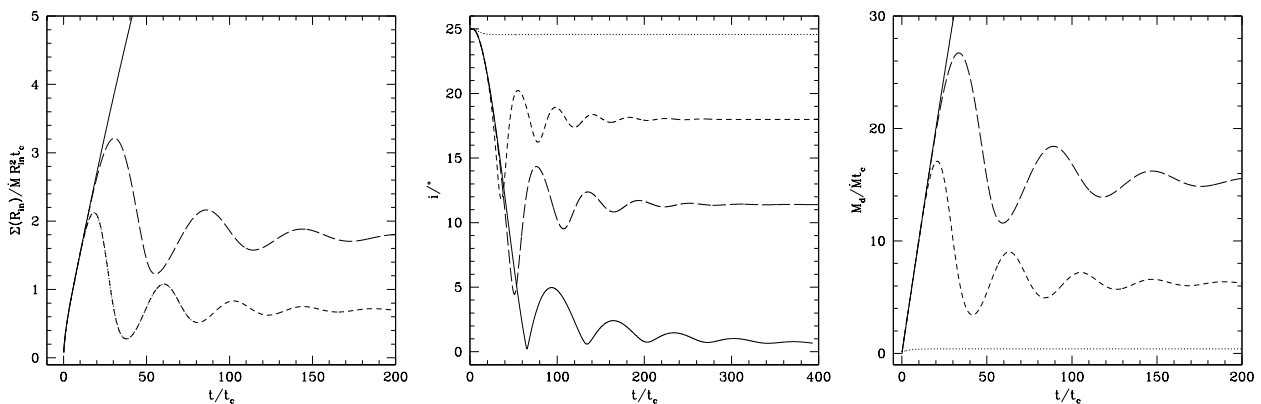


Figure 6. Discs with $R_{\text{tid}} = 20 R_*$. Left: The surface density at the inner edge of the disc. Middle: The inclination of the inner edge of the disc. Right: The total mass of the disc. In each plot the dotted line shows a disc with $\Sigma_* = 0$ (not shown in the left plot because it is zero). The solid line shows a disc with $v_R = 0$ inner boundary condition. The dashed lines show discs with the varying inner boundary condition with $K = 10$ (long-dashed lines) and $K = 100$ (short dashed lines).

of the disc. Even if there is no observed misalignment for a Be star system, the formation mechanism of the companion neutron star by an asymmetric supernova did most probably produce a misalignment (Martin, Tout & Pringle 2009). There is a large range of orbital periods and eccentricities in the Be/B star binaries.

Ideally we should make an individual model of each system in order to draw firm conclusions about its evolution. However, in this Section we just consider the general properties of the Be star systems. We choose the mass of the Be star according to its spectral type (see Eggleton, Tout & Fitchett 1989) and then find the corre-

sponding stellar radius from the mass (e.g. Tout et al. 1996). We list the properties in Table 2.

In Table 3 we show the disc properties in each Be star binary. We find the semi-major axis of the orbit from equation (24) and then the periastron separation is $p = (1 - e)a$. We find the average separation with equation (29). The tidal warp radius is found with equation (30) with $n = 4$ and then the tidal timescale with equation (32). The tidal timescale tells us the timescale on which the disc reaches steady state, as shown in Section 4.4. Any oscillations of the disc mass and inner inclination of the disc occur on a timescale shorter than this.

| Be/B Star Binary | a/R_* | p/R_* | \bar{R}_b/R_* | R_{tid}/R_* | $t_{\text{tid}*}/\text{yr}$ |
|--------------------------|---------|---------|-----------------|----------------------|-----------------------------|
| 4U0115+634 (V635 Cas) | 9.3 | 6.2 | 8.8 | 8.2 | 2.1 |
| 59 Cyg | 11.7 | 9.3 | 11.4 | 12.7 | 3.4 |
| J0045-7319 | 17.4 | 3.3 | 10.2 | 10.2 | 3.3 |
| A0535+262 (V725 Tau) | 25.7 | 13.6 | 22.6 | 54.4 | 36.5 |
| 0053+604 (γ Cas) | 38.5 | 28.5 | 37.2 | 146.6 | 161.4 |
| 28 Tau | 67.1 | 26.8 | 53.6 | 93.7 | 44.9 |
| SS 2883 (B1259-63) | 165 | 21.4 | 81.2 | 554.5 | 825.2 |

Table 3. The binary Be/B star binaries shown in Table 1 that have measured period and eccentricity. Here we compute the binary semi-major axis, a , the periastron separation, p , the average radius, \bar{R}_b , the tidal warp radius, R_{tid} and the tidal timescale at R_* . We choose the mass and radius of the Be star system depending on its spectral type from Table 1.

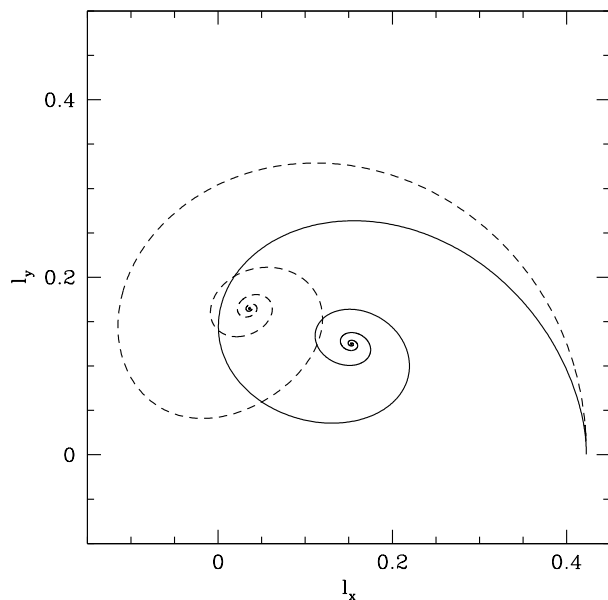


Figure 7. The evolution of the inner (solid line) and outer (dashed line) angular momenta of the disc with the varying inner radial velocity inner boundary condition with $K = 10$ and $R_{\text{tid}} = 20 R_*$. At $t = 0$ the disc begins with $l_y = 0$ on the right hand side of the plot.

The systems V635 Cas and 59 Cyg should have an evolution similar to that described by Fig. 4 as they both have small tidal warp radii. The mass and inner disc inclination evolution is similar to the dotted line in Fig. 5. They have tidal timescales of a few years and so should reach a steady state disc relatively quickly. The oscillations in mass and inner disc inclination should be minimal if the accretion rate on to the Be star decretion disc is constant. However, if the mass ejection rate from the Be star is not constant then the warping and precession could continue over time.

Negueruela et al. (2001) observed the Be/X-ray transient 4U0115+63/V635 Cas in optical, infrared and X-rays and that the disc warps, tilts and starts precessing. They found a quasi-period cycle with a period of 3–5 yr on which the Be star disc forms, grows and is lost. They observed two Type II outbursts before the disc became faint. The H α line profile in this system is usually double peaked. However, just before the outbursts, the line became single peaked and

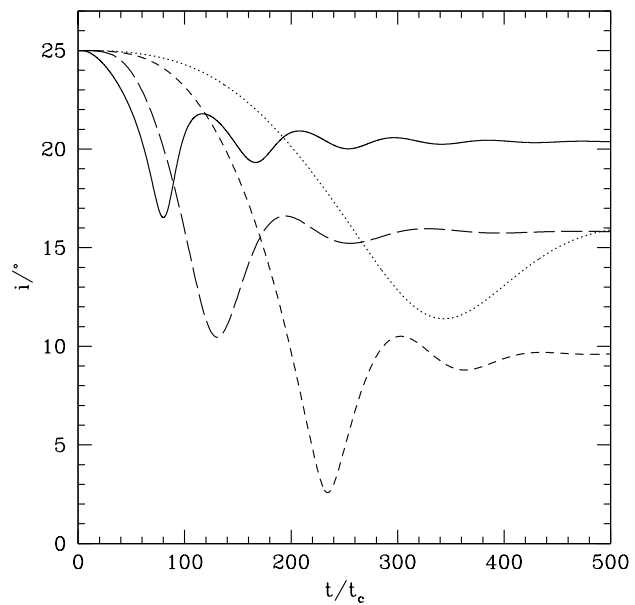


Figure 8. The inner disc inclination evolution for models with $R_{\text{tid}} = 40 R_*$ and $K = 100$. The solid line has $\alpha_2/\alpha_1 = 0.1$ and $n = 4$. The long-dashed line has $\alpha_2/\alpha_1 = 0.1$ and $n = 7/2$. The short dashed line has $\alpha_2/\alpha_1 = 0.02$ and $n = 7/2$. The dotted line has $\alpha_2/\alpha_1 = 0.1$ and $n = 3$.

this was sometimes followed by a shell event. They assume that the warping is because the disc becomes unstable to radiation driven warping. However, in such a short period binary with only a moderate eccentricity the tidal torques will certainly cause the disc to warp and precess if the system is misaligned. As the warped disc precesses, the line profile changes shape. Negueruela et al. (2001) suggest that the warped parts of the disc will have a strong interaction with a fast stellar wind and stellar irradiation and so a large amount of gas falls on to the neutron star causing a Type II outburst and then the disc becomes faint because it has lost a lot of mass. We have found that the tidal timescale in the inner parts of the disc is about 2.1 years. This is the timescale on which the disc would reach steady state or else its maximum warping if the accretion on to the disc from the star is at a constant rate. However, with a varying mass ejection rate from the Be star, the disc will continue to warp and precess as the mass in the disc varies.

| Be Star System Properties | | | | |
|---|---------------|-----|----|-----|
| Be Star | | | | |
| Spectral Type | B0 | B1 | B2 | B8 |
| Mass M_1/M_\odot | 17 | 15 | 12 | 2.9 |
| Radius R_\star/R_\odot | 10 | 8.5 | 7 | 3.7 |
| Mass of Neutron Star, M_2 | | | | |
| | 1.4 M_\odot | | | |
| Disc Scale Height (H_\star/R_\star) | | | | |
| | 0.04 | | | |

Table 2. Properties of the Be star systems we choose. We use the B0 star parameters throughout the work and the other parameters for Table 3.

The B-star binary PSR J0045–7319 has a spin-orbit misalignment suggested by its orbital plane precession (Kaspi et al. 1996; Lai, Bildsten & Kaspi 1995). In this case the B star rotates retrogradely with respect to the orbit (Lai 1996). The system has a tidal timescale of 3.3 yr. This system should show oscillations in its mass and inner disc inclination on the timescale of a year or so if a disc was ejected.

Haigh, Coe & Fabregat (2004) found that the disc in A0535+26 grows and decays on a quasi-cycle period of about 1500 d by observing the change in quantised, IR excess flux states. The system has also shown type II outbursts in 1994 and 2005 (Coe et al. 2006). Because the system has only a moderate eccentricity, unless it has a very large misalignment angle, the disc will be truncated by tidal torques before it can reach the orbit of the neutron star. We find the tidal timescale in this system to be around 37 years and because the tidal warp radius is large, oscillations in mass and inclination should occur on a timescale of around the order of 10 years.

The Be star ζ Tau has a companion that is yet to be detected. Because the eccentricity is unknown we do not compute the tidal timescales but note that the system may be similar to A0535+26. Recently Schaefer et al. (2010) used interferometry to observe the disc and suggested that the tilt of the disc is precessing.

γ Cas showed two successive shell phases over a period of 6 years (Hummel 1998). We find the tidal timescale at the inner edge of the disc to be 161 years. The tidal warp radius is very large, at $147 R_\star$. This implies that the system will undergo large oscillations in disc mass and inner disc inclination as the disc mass builds up.

Hirata (2007) use polarimetry to observe the precession in 28 Tau (Pleione). Over the course of a hundred years, the star has changed from Be \rightarrow B, shell \rightarrow Be, shell \rightarrow Be with an activity cycle of 35 yr. It is currently in the Be phase. They find that over the time period 1974 to 2003 the disc axis precessed from 60° to 130° . With the H α profile they suggest that the disc inclination has also changed drastically. They found the precession period of 28 Tau to be 80.5 yr but assumed a constant precession rate. Our model predicts that the precession period is 45 yr. The rigid body precession model of Larwood (1998) found that the precession period is 270 yr and 70 yr for disc radii of $10 R_\star$ and $25 R_\star$ respectively, also in reasonable agreement.

The tidal torque from the companion will have an effect on all of the Be stars in listed in Table 3 apart from maybe SS2883 which has the longest orbital period and a

very large eccentricity. The timescale on which the averaged tidal torque acts is very long. Because of the large eccentricity, a one armed spiral structure may form at periastron passage (Hayasaki & Okazaki 2004, 2005). The fact that tidal torques are negligible in this system has been noted before by Kochanek (1993); Manchester et al. (1995); Lai, Bildsten & Kaspi (1995). Wex et al. (1998) suggests that the solution is a precessing orbit caused by the quadrupole moment of the tilted companion star.

6 CONCLUSIONS

We find that in Be star discs the torques from a neutron star companion are important and the discs can become warped and twisted if the system is misaligned (except in the systems with the longest periods). Even though Be star’s have eccentric orbits with their companions, the orbital period is short compared the timescale on which the tidal torque acts and so we can average the tidal torque over an orbital period. The discs are truncated at a radius smaller than the periastron separation of the binary providing the the eccentricity is not close to 1 and the misalignment is not too large. The size of the disc decreases with increasing eccentricity of the binary orbit. In most systems, it is unlikely that the neutron star will pass through the disc and so Type II outbursts are more likely linked to the warping of the disc.

We have made numerical models of Be star discs that are assumed to be truncated by the companion and considered solutions with three different inner boundary conditions that approximate the magnetic torque from the Be star. First we considered a magnetic torque strong enough to prevent all accretion back on to the Be star, or zero radial velocity. In this case the disc mass increases linearly in time and the disc tends towards complete alignment with the binary orbital plane. Secondly we considered a disc with a zero torque inner boundary condition normally associated with accretion discs. The surface density at the inner edge of the disc is zero and the disc has a small mass. The disc moves towards a steady state solution with the inner parts close to alignment with the equator of the Be star and the outer parts become warped towards the binary plane but shows little precession.

Finally we considered a magnetic torque that is strongest at the equator of the Be star (where it rotates fastest) and decreases as the disc moves away from there. The corresponding boundary condition varies the radial velocity at the inner edge of the disc with the inclination to the Be star equator. The mass addition and tidal torques oscillate in dominance as the surface density varies. A warped and twisted steady state is reached once the oscillations die away on the tidal timescale at the inner edge of the disc which is of the order of a year up to a few hundred years (see Table 3). On a timescale shorter than this the disc mass and inclination oscillate if the tidal warp radius is large. We suggest that these oscillations could be the cause of the shell events. The inclination and mass of the disc change on a timescale of a few, to a few tens of years until the disc reaches its steady state. If Type II X-ray outbursts are caused by a warped disc interacting with a fast stellar wind then the tidally warped disc solution could provide warping on a timescale similar to those observed. If the disc under-

goes periodic mass ejections followed by a decay of the disc mass, then the angular momentum distribution can be reset to being small and aligned with the Be star spin. As the disc mass builds up each time the oscillations will be observed.

Observers should try to measure the misalignment between the spin of the Be star and the binary orbital plane of more Be star systems. We note that the inclination of the disc is not necessarily aligned with either the binary orbit or the spin of the Be star and so the two planes need to be measured independently of the disc inclination.

ACKNOWLEDGEMENTS

We thank Phil Charles for useful conversations. RGM thanks the Space Telescope Science Institute for a Giacconi Fellowship

REFERENCES

- Artymowicz P., Lubow S. H., 1994, *ApJ*, 421, 651
- Bjorkman J. E., The Be Phenomenon in Early-Type Stars, IAU Colloquium 175, ASP Conference Proceedings, eds Smith M. A., Henrichs H. F., San Francisco, 2000, 214, 435
- Bjorkman J. E., Cassinelli J. P., 1993, *ApJ*, 409, 429
- Bjorkman K. S., Miroshnichenko A. S., McDavid D., Pogrosheva T. M., 2002, *ApJ*, 573, 812
- Cassinelli J. P., MacGregor K. B., 2000, in IAU Colloq. 175, The Be Phenomenon in Early-Type Stars, ed. Smith M. A., Henrichs M. F., Fabregat J., (ASP Conf. Ser. 214; San Francisco: ASP), 337
- Cassinelli J. P., Brown J. C., Maheswaran M., Miller N. A., Telfer D. C., 2002, *ApJ*, 578, 951
- Coe M. J., Reig P., McBride V. A., Galache J. L., Fabregat J., 2006, *MNRAS*, 368, 447
- Dougherty S. M., Waters L. B. F. M., Burki G., Coté J., Cramer N., van Kerkwijk M. H., Taylor A. R., 1994, *A&A*, 290, 609
- Eggleton P. P., Tout, C. A., Fitchett M. J., 1989, *ApJ*, 347, 998
- Grundstrom E. D., Gies D. R., 2006, *ApJ*, 651, L53
- Haigh N. J., Coe M. J., Fabregat J., 2004, *MNRAS*, 350, 1457
- Hanuschik, R. W., 1996, *A&A*, 308, 170
- Harmanec P. 1984, *Bull. Astron. Inst. Czechoslovakia*, 35, 164
- Harmanec P., Habuda P., Štefl S., et al., 2000, *A&A*, 364, L85
- Harmanec P., Božić H., Percy J. R., et al., 2002, *A&A*, 387, 580
- Hayasaki K., Okazaki A. T., 2004, *MNRAS*, 350, 971
- Hayasaki K., Okazaki A. T., 2005, *MNRAS*, 360 L15
- Holman M., Touma J., Tremaine S., 1997, *Nat*, 386, 254
- Hughes A., Bailes M., 1999, *ApJ*, 522, 504
- Hutchings J. B., 1984, *PASP*, 96, 312
- Hirata R., Active OB-Stars: Laboratories for Stellar and Circumstellar Physics, eds. Okazaki A. T., Owocki S. P., Štefl S., 2007, *ASPC*, 361, 267
- Hummel W., 1998, *A&A*, 330, 243
- Ichikawa S., Osaki Y., 1994, *PASJ*, 46, 621
- Jones C. E., Sigut T. A. A., Porter J. M., 2007, *MNRAS*, 386, 1922
- Jones C. E., Sigut T. A. A., Porter J. M., 2008, *MNRAS*, 386, 1922
- Katahira J., Hirata R., Ito M., Katoh M., Ballereau D., Chauville J., 1996, *PASJ*, 39, 329
- Kaspi V. M., Bailes M., Manchester R. N., Stappers B. W., Bell J. F., 1996, *Nat*, 381, 584
- Kochanek C. S., 1993, *ApJ*, 406, 638
- Larwood J., 1998, *MNRAS*, 299, L32
- Lai D., Bildsten L., Kaspi V. M., 1995, *ApJ*, 452, 819
- Lai D., 1996, *ApJ*, 466, L35
- Larionov V., Lyuty V. M., Zaitseva G. V., 2001, *A&A*, 378, 837
- Lee U., Saio H., Osaki Y., 1991, 250, 432
- Livio M., Pringle J. E., 1992, *MNRAS*, 259, 23
- Lodato G., Price D. J., 2010, *MNRAS*, 405, 1212
- Lubow S. H., Ogilvie G. I., 2000, *ApJ*, 538, 326
- Manchester R. N., Johnston S., Lyne A. G., D'Amico N., Bailes M., Nicastro L., 1995, *MNRAS*, 280, L31
- Martin R. G., Pringle J. E., Tout C. A., 2007, *MNRAS*, 381, 1617
- Martin R. G., Tout C. A., Pringle J. E., 2008, *MNRAS*, 387, 188
- Martin R. G., Tout C. A., Pringle J. E., 2009, *MNRAS*, 397, 1563
- Martin R. G., Pringle J. E., Tout C. A., 2009, *MNRAS*, 400, 383
- Martin R. G., Lubow S. H., 2011, arXiv1012.4102
- Negueruela I., Reig P., Coe M. J., Fabregat J., 1998, *A&A*, 336, 251
- Negueruela I., Reig P., Finger M. H., Roche P., 2000, *A&A*, 356, 1003
- Negueruela I., Okazaki A. T., Fabregat J., Coe M. J., Munari U., Tomov T., 2001, *A&A*, 369, 117
- Ogilvie G. I., 1999, *MNRAS*, 304, 557
- Ogilvie G. I., Dubus G., 2001, *MNRAS*, 320, 485
- Okazaki A. T., 2001, X-ray Astronomy 2000, eds Giacconi R., Serio S., Stella L., ASP Conference Series, 324, 281
- Okazaki A. T., Bate M. R., Ogilvie G. I., Pringle J. E., 2002, *MNRAS*, 337, 967
- Okazaki A. T., 2007, Active O-B Stars: Laboratories for Stellar and Circumstellar Physics, ASP Conference Series, eds Štefl S., Owocki S. P., Okazaki A. T., 361, 230
- Okazaki A. T., Hayasaki K., 2007, Active O-B Stars: Laboratories for Stellar and Circumstellar Physics, ASP Conference Series, eds Štefl S., Owocki S. P., Okazaki A. T., 361, 395
- Okazaki A. T., 2007, Massive Stars in Interacting Binaries, eds St-Louis N., Moffat A. F. J., ASP Conference Series, 367, 485
- Owocki S. P., ud Doula A., 2003, in Magnetic Fields in O, B and A Stars: Origin and Connection to Pulsation, Rotation and Mass Loss, eds Balona L. A., Henrichs H. F., Medupe R., ASP, San Francisco, 305, 350
- Paczyński B., 1977, *ApJ*, 216, 822
- Papaloizou J. C. B., Lin D. N. C., 1984, *ApJ*, 285, 818
- Porter J. M., 1996, *MNRAS*, 280, L31
- Porter J. M., 1997, *A&A*, 324, 597
- Porter J. M. 1999, *A&A*, 348, 512
- Porter J. M., 2003, *Be Star Newsl.*, 36, 6
- Porter J. M., Rivinius T., 2003, *PASP*, 115, 1153

- Pringle J. E., 1981, *ARA&A*, 19, 137
 Pringle J. E., 1991, *MNRAS*, 248, 754
 Pringle J. E., 1992, *MNRAS*, 258, 811
 Quirrenbach A., Bjorkman K. S., Bjorkman J. E., et al., 1997, *ApJ*, 479, 477
 Rajoelimanana A. F., Charles P. A., Udalski A., 2010, *arXiv1012.4610R*
 Rappaport S., Clark G. W., Cominsky L., Li F., Joss P. C., 1978, *ApJ*, 224, L1
 Rivinius T., Štefl S., 2000, *The Be Phenomenon in Early-Type Stars*, ed. M. Smith, H. Henrichs, J. Fabregat, IAU Col., 175, 581
 Schaefer G. H., Gies D. R., Monnier J. D., et al., 2010, *AJ*, 140, 1838
 Shakura N. I., Sunyaev R. A., 1973, *A&A*, 24, 337
 Steele I. A., Negueruela, I., Coe, M. J., Roche, P. 1998, *MNRAS*, 297, L5
 Stella L., White N. E., Rosner R., 1986, *ApJ*, 208, 669
 Telting J. H., Waters L. B. F. M., Roche P., Boogert A. C. A., Clark J. S., de Martino D., Persi P., 1998, *MNRAS*, 296, 785
 Tout C. A., Pols O. R., Eggleton P. P., Han Z., 1996, *MNRAS*, 281, 257
 Waters L. B. F. M., Cote J., Lamers H. J. G. L. M., 1987, *A&A*, 185, 206
 Wex N., Johnston S., Manchester R. N., Lyne A. G., Stappers B. W., Bailes M., 1998, *MNRAS*, 298, 997
 Wood K., Bjorkman K. S., Bjorkman J. E., 1997, *ApJ*, 477, 926

APPENDIX A: INNER BOUNDARY CONDITIONS

Here we consider the torque on the inner parts of the disc from the rotating Be star. The torque may be created by the magnetic field of the star (e.g., Livio & Pringle 1992). We need only consider a flat disc to investigate the inner surface density boundary condition because we have chosen the angular momentum to satisfy $\partial l / \partial R = 0$. The surface density evolution equation for a flat disc with a source of angular momentum is

$$\frac{\partial \Sigma}{\partial t} = \frac{1}{R} \frac{\partial}{\partial R} \left[3R^{\frac{1}{2}} \frac{\partial}{\partial R} \left(\nu_1 \Sigma R^{\frac{1}{2}} \right) \right] - \frac{1}{R} \frac{\partial}{\partial R} \left[\frac{2\Lambda \Sigma R^{\frac{3}{2}}}{\sqrt{GM_1}} \right], \quad (\text{A1})$$

(Pringle 1991), where the input rate of angular momentum per unit mass is

$$\Lambda = \frac{GM_1}{R} f \quad (\text{A2})$$

and $f(R) \leq 1$ measures the strength of the torque (Pringle 1991). The function f is a strongly decreasing function of radius (Papaloizou & Lin 1984; Pringle 1991). The radial velocity in the disc is

$$v_R = \frac{2\sqrt{GM_1}}{R^{\frac{1}{2}}} f - \frac{3}{\Sigma R^{\frac{1}{2}}} \frac{\partial}{\partial R} \left(\nu_1 \Sigma R^{\frac{1}{2}} \right). \quad (\text{A3})$$

We can rearrange this to find

$$f = \frac{R^{\frac{1}{2}}}{2(GM_1)^{\frac{1}{2}}} \left[v_R + \frac{3}{\Sigma R^{\frac{1}{2}}} \frac{\partial}{\partial R} \left(\nu_1 \Sigma R^{\frac{1}{2}} \right) \right]. \quad (\text{A4})$$

A1 Zero Radial Velocity

First we consider a torque that is strong enough to prevent all accretion back on to the star. This is equivalent to the inner boundary condition $v_R = 0$ at $R = R_*$ no matter what the inclination of the inner parts of the disc relative to the Be star spin. In this case with equation (A3) we find the torque must be such that

$$f = \frac{3}{2\sqrt{GM_1}\Sigma} \frac{\partial}{\partial R} \left(\nu_1 \Sigma R^{\frac{1}{2}} \right) \quad (\text{A5})$$

and because f falls off quickly with radius, this is approximately equivalent to $f = 0$ and

$$\frac{\partial}{\partial R} \left(\nu_1 \Sigma R^{\frac{1}{2}} \right) \Big|_{R=R_*} = 0. \quad (\text{A6})$$

We can replace the source term in equation (A1) with this boundary condition.

A2 Zero Torque

Next we consider a disc with a zero torque inner boundary condition. We can choose $f = 0$ and then the torque on the disc is the usual viscous torque

$$T = -3\pi\nu_1\Sigma(GM_1R)^{\frac{1}{2}}. \quad (\text{A7})$$

For zero torque at the inner edge we have $\Sigma = 0$ at $R = R_*$.

A3 Varying Inner Radial Velocity

The Be star rotates fastest at the equator. The third torque we consider varies with the inclination of the inner parts of the disc. The torque is strongest at the equator and falls off as the disc moves away from the equator. We choose a torque of the form

$$f = C \left(\frac{R}{R_*} \right)^{-10} \exp \left[\frac{-(i_* - \theta)^2}{\delta^2} \right], \quad (\text{A8})$$

where C and δ are constant. We can vary the rate at which the torque falls off away from the equator of the Be star and the torque falls off quickly with radius from the star.

If the constant, C , is large enough, this is equivalent to an inner boundary condition that takes $v_R = 0$ only at the equator, when the star rotates at break up, but allows for accretion on to the Be star as the inclination of the inner disc moves away from the equator of the Be star. At the equator $i_* = \theta$. As the inner disc inclination moves towards the pole, the viscous torque tends to zero and $\Sigma_* = 0$ and $v_R \rightarrow \infty$. Hence we can parametrise the radial velocity at the inner edge of the disc as

$$v_{R*} = -3K \frac{\nu_{1*}}{R_*} \left[\frac{\Omega_*/\Omega_{\text{star}}}{\cos(i_* - \theta)} - 1 \right], \quad (\text{A9})$$

where K is a dimensionless constant that we can vary. We cannot determine K without looking in more detail at the boundary layer between the disc and the star. The rotation rate of the Be star is Ω_{star} and the Keplerian rotation rate

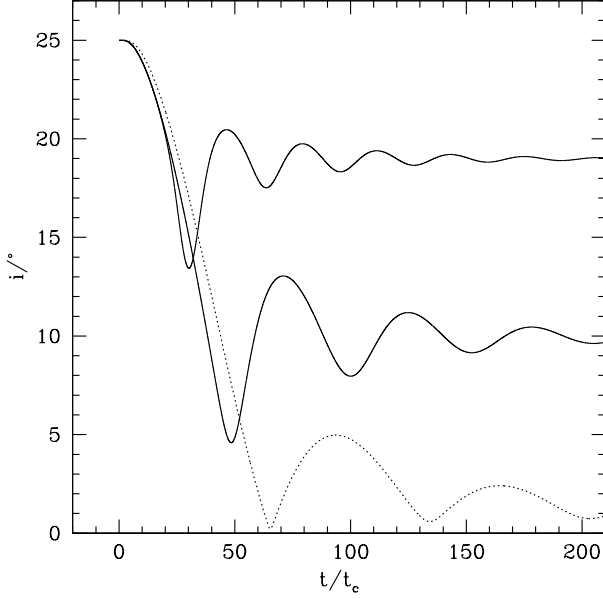


Figure A1. A disc with $R_{\text{tid}} = 20 R_*$ including the additional torque term given in equation A8 and an inner boundary condition $\Sigma(R_*) = 0$. We take the constant $C = 15$ and the upper solid line has $\delta = 0.1$ and the lower line has $\delta = 0.4$. The dotted line shows the case with the inner boundary condition $v_R = 0$ for comparison (the solid line in the middle plot of Fig. 6).

of the inner parts of the disc is $\Omega_* = \Omega(R_*)$. The boundary condition at the inner edge of the disc is

$$\frac{\partial}{\partial R}(\nu_1 \Sigma R^{\frac{1}{2}}) \Big|_{R=R_*} = K \frac{\nu_{1*} \Sigma_*}{R_*^{\frac{1}{2}}} \left[\frac{\Omega_*/\Omega_{\text{star}}}{\cos(i_* - \theta)} - 1 \right] \quad (\text{A10})$$

for $\cos(i_* - \theta) \neq 0$. If the star is rotating at break up then $\Omega_{\text{star}} = \Omega_*$.

In Fig. A1 we plot the inclination of the inner edge of the disc as a function of time for a disc with $R_{\text{tid}} = 20 R_*$ including the varying torque in equation (A8) and an inner boundary condition of $\Sigma(R_*) = 0$. We see that this torque does indeed reproduce a similar behaviour to that with the varying inner boundary condition that we describe in Section 4.4. The inner boundary condition is an approximation to the torque from a Be star that varies with height above the equator. However, the constants, C , δ and K can only be determined by looking in more detail at the magnetic torque term.